Self-consistent electronic subband structure of undoped InAs/GaSb-based type II and broken-gap quantum well systems

W. Xu[a)]
Institute of Solid State Physics, Chinese Academy of Sciences, Hefei 230031, China and Department of Theoretical Physics, Research School of Physical Sciences and Engineering, Australian National University, Canberra, ACT 0200, Australia

P. A. Folkes
U.S. Army Research Laboratory, Adelphi, Maryland 20783

Godfrey Gumbs
Department of Physics, Hunter College, City University of New York, New York 10021

(Received 22 April 2007; accepted 19 June 2007; published online 1 August 2007)

Motivated by a very recent experimental work on investigating electronic properties of InAs/GaSb-based type II and broken-gap quantum well structures, in this article we present a simple and transparent theoretical approach to calculate electronic subband structure in such device systems. The theoretical model is developed on the basis of solving self-consistently the Schrödinger equation for the eigenfunctions and eigenvalues coupled with the Poisson equation for the confinement potentials, in which the effects such as charge distribution and depletion are considered. In particular, we examine the effect of a GaSb cap layer on electronic properties of the quantum well systems in conjunction with experiments and experimental findings. The results obtained from the proposed self-consistent calculation can be used to understand important experimental findings and are in line with those measured experimentally. © *2007 American Institute of Physics*.
[DOI: 10.1063/1.2759873]

I. INTRODUCTION

Proposed theoretically in 1983 (Ref. 1) and realized experimentally first in 1987,[2] InAs/GaSb-based type II and broken-gap quantum well (QW) and superlattice systems have been promised as advanced electronic and optical devices including negative persistent photoconductors,[3] intrinsic excitonic devices,[4] semimetallic heterostructures,[5] infrared lasers,[6] subterahertz photovoltaic devices,[7] to name but a few. Such QW systems have some very interesting and unique features for electronic subband structure and the corresponding electronic and optoelectronic properties. (1) The conducting electrons and holes are separated spatially in two adjacent layers (often referred to as type II structure), i.e., in InAs and GaSb layers respectively. (2) The top of the valence band for the hole layer E_v^{GaSb} is significantly higher than the bottom of the conduction-band for the electron layer E_c^{InAs} (often referred as broken-gap system), i.e., $E_v^{\mathrm{GaSb}}-E_c^{\mathrm{InAs}} \sim +150$ meV. (3) Both electron and hole subbands in different layers are occupied, respectively, by electrons and holes so that a two-dimensional electron gas (2DEG) and a 2D hole gas (2DHG) are formed in the InAs and GaSb layers, respectively. These features are in sharp contrast to a conventional QW in which the electrons and holes are confined within the same material layer and the conduction band is always higher than the valence band so that only electron subbands (or hole subbands) are populated for a *n*-type (or *p*-type) structure.

Over the last two decades, intensive theoretical research has been carried out in studying the electronic subband structure of InAs/GaSb-based type II and broken-gap QW systems using techniques such as the $\mathbf{k}\cdot\mathbf{p}$ band-structure calculations on the basis of the Luttinger Hamiltonian[1,8] and Burt's Hamiltonian,[9] pseudopotential plane-wave approach,[5] tight-bindinglike effective-bond-orbit model,[6] etc. These state-of-the-art condensed matter theories have already provided us with a clear picture of the electronic subband structure for such novel QW systems. At present, important sample parameters (e.g., effective masses for electrons and holes, dispersion relation of the energy spectra for electrons and holes, conduction and valence band offsets and edge discontinuities, overlap of the InAs conduction band with the GaSb valence band, etc.) have been obtained from these calculations, which agree well with those determined experimentally. However, in these band-structure calculations the important consequences from a real sample device, such as charge distribution, donor or acceptor doping, background impurities, charge depletion, etc., have often been neglected. From a viewpoint of device application, it is also important and necessary to be able to know how electronic properties in an InAs/GaSb-based type II and broken-gap QW (such as electron and hole subband energies, electron and hole densities, charge distributions, and depletion density and length) vary with the sample-growth parameters (such as the widths of the InAs and GaSb well layers, doping position and concentration, and the presence of the cap layers). In particular, in sharp contrast to a conventional QW in which the conducting carriers come mainly from the ionization of doped impurities, once a type II and broken-gap QW is achieved both 2DEG and 2DHG can coexist in different layers in equilib-

a)Electronic address: wen105@rsphysse.anu.edu.au

rium even without intentional doping. In such a case, the density of the 2DEG may differ from that of the 2DHG and, therefore, the charge distribution required by the condition of charge number conservation can affect significantly the electronic properties of the sample system. Hence, to have an in-depth understanding of the electronic properties in a type II and broken-gap QW, there is a need for developing a theoretical approach to examine how electronic subband structure varies with sample-growth parameters in such QW systems. It was demonstrated in the past[10–14] that by solving self-consistently the Schrödinger equation for the eigenfunctions and eigenvalues in conjunction with the Poisson equation for the confinement potential, the self-consistent calculation for electronic subband structure in QW systems can be carried out by taking into account of the effects such as impurity doping, charge distribution, band bending, the presence of a gate voltage, etc. In this article, in conjunction with our very recent experimental findings[15] we develop a transparent approach to calculate self-consistently the electronic subband structure in InAs/GaSb-based type II and broken-gap QW systems.

From a fundamental perspective, up to now many well-known features for a conventional QW (C-QW) remain unknown for a type II and broken-gap QW (T2BG-QW). For example, it is known that in a doped C-QW at low temperatures, the Fermi level of the system is pinned at the impurity level so that the conducting carriers come mainly from the ionization of the doping impurities. However, in an undoped AlSb/InAs/GaSb-based T2BG-QW in the presence of a GaSb cap layer, it is not clear whether the Fermi level is predominantly determined by the intrinsic bulk donor defects in GaSb (AlSb) barriers or by the extrinsic surface defects in the cap layer. It is not well understood if the Fermi level still pins at the impurity level or not. Furthermore, if the pinning of the Fermi energy at the impurity level still holds in a T2BG-QW, should it be pinned at the donor level, or acceptor level, or surface-defect level since both electron and hole states are occupied and the 2DEG and 2DHG are formed in different layers? Very recently, we have carried out a systematic experimental study on electronic properties of InAs/GaSb-based T2BG-QW systems using magnetotransport measurements.[15] Through examining the dependence of electron and hole densities in the system on the thickness of a GaSb cap layer, we found that in an undoped sample structure with a narrow GaSb well layer, the Fermi level of the system is mainly determined by bulk donor defects in the AlSb barrier layer adjacent to the InAs well layer. As the width of the GaSb cap layer increases, the Fermi energy varies slightly due to band bending induced by charge depletion and by the injection of carriers from the cap layer. The results obtained from the self-consistent calculation confirmed these findings[15] and reproduced those measured experimentally. In this article, we present the theoretical component of the investigation. In Sec. II, a detailed theoretical consideration is described to figure out the model calculation in conjunction with experiments and experimental findings. In Sec. III, we present numerical results obtained from the self-consistent calculation and discuss important features of the electronic subband structure in undoped T2BG-QW systems. The main conclusions drawn from this study are summarized in Sec. IV.

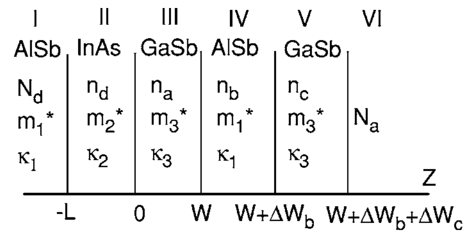

FIG. 1. Schematic diagram of the sample structure. Here, m_i^* and κ_i are respectively the effective mass and static dielectric constant for different material layers, N_i and n_i are background or doped impurity concentrations.

II. THEORETICAL CONSIDERATIONS AND APPROACHES

From a theoretical point of view, self-consistent calculation is a powerful and practical tool in calculating electronic properties in a QW as a function of known material coefficients and sample-growth parameters and in studying and assessing the real device systems. We have successfully applied the approach of the self-consistent calculation to the investigation of δ-doped AlGaAs/GaAs single QWs,[10] modulation-doped AlGaAs/GaAs double QWs,[11] modulation-doped AlGaAs/GaAs QWs in the presence of parallel[12] and perpendicular[13] magnetic fields, and modulation-doped AlGaAs/InGaAs/GaAs QWs.[14] In the present study, we generalize these well-developed theoretical approaches to calculate self-consistently the electronic subband structure in InAs/GaSb-based type II QW structures.

Here we consider a typical sample structure grown along the z direction (see Fig. 1): (i) an AlSb layer in I ($z<-L$) is to form a barrier for electrons; (ii) the 2DEG is formed in an InAs well layer with a width L in II ($-L<z<0$); (iii) the 2DHG is located within a GaSb well layer with a width W in III ($0<z<W$); (iv) an AlSb layer with a thickness ΔW_b in IV ($W<z<W+\Delta W_b$) is to form a barrier for holes; (v) a GaSb cap layer with a thickness ΔW_c in V ($W+\Delta W_b<z<W+\Delta W_b+\Delta W_c$) is grown to provide an extra source of charges in the system; and (vi) a layer shows the native oxide at the GaSb cap layer surface ($z>W+\Delta W_b+\Delta W_c$). For a sample structure as shown in Fig. 1, the dielectric constant $[\kappa(z)]$ and the effective mass $[m^i(z)]$ for an electron or a hole in different material layers are, respectively

$$[\kappa(z),m^i(z)]=\begin{cases}(\kappa_1,m_1^i), & \text{I;}\\(\kappa_2,m_2^i), & \text{II;}\\(\kappa_3,m_3^i), & \text{III;}\\(\kappa_1,m_1^i), & \text{IV;}\\(\kappa_3,m_3^i), & \text{V,}\end{cases} \quad (1)$$

with $i=e(i=h)$ for an electron (a hole). In the present study, for simplicity we use the known material parameters to calculate the electronic subband structure under the usual effective-mass approximation. In doing so, the single-particle Schrödinger equation for an electron (or a hole) is given as

$$\left[-\frac{\hbar^2}{2}\frac{d}{dz}\frac{1}{m^i(z)}\frac{d}{dz}+U_i(z)-\varepsilon_n^i\right]\psi_n^i(z)=0, \tag{2}$$

where the confinement potential energy for an electron (or a hole) is

$$U_i(z)=U_H(z)+U_{ex}^i(z)+\Delta E_i(z). \tag{3}$$

The conduction- and valence-band off sets in different layers are, respectively

$$[\Delta E_c(z),\Delta E_v(z)]=\begin{cases}(2000\ \text{meV},-300\ \text{meV}), & \text{I};\\(0\ \text{meV},-450\ \text{meV}), & \text{II};\\(960\ \text{meV},145\ \text{meV}), & \text{III};\\(2000\ \text{meV},-300\ \text{meV}), & \text{IV};\\(960\ \text{meV},150\ \text{meV}), & \text{V},\end{cases} \tag{4}$$

which are measured from the bottom of the conduction band in the InAs layer in the absence of many-body interactions. Because there is no density-functional theory for T2BG-QW structures to date, we do not know the exchange and correlation energy in such systems. We therefore take into account only the exchange potential energy in the calculation, which is for electrons (or holes)

$$U_{ex}^i(z)=-0.0783\frac{e^2}{\kappa(z)}[n_i(z)]^{1/3}, \tag{5}$$

with $n_i(z)$ being the electron (or hole) distribution along the growth direction. The Hartree potential seen by electrons and holes is determined by the Poisson equation

$$\frac{d}{dz}\kappa(z)\frac{d}{dz}U_H(z)=-e\rho(z), \tag{6}$$

where the charge distribution is given by (see Fig. 1)

$$\rho(z)=-e\begin{cases}\Delta n(z), & \text{I}_1{:}z\le -L-L_d;\\\Delta n(z)-N_d, & \text{I}_2{:}-L-L_d<z\le -L;\\\Delta n(z)-n_d, & \text{II};\\\Delta n(z)+n_a, & \text{III};\\\Delta n(z)+n_b, & \text{IV};\\\Delta n(z)+n_c, & \text{V},\end{cases} \tag{7}$$

with $\Delta n(z)=n_e(z)-n_h(z)$. Here, we have considered a sample without intentional doping so that background impurities in regimes II, III, IV, and V in Fig. 1 are all ionized. We assume that the background impurities in the layer II (i.e., n_d in $-L<z<0$) behave like donors and those in the layer III, VI, and V (i.e., n_a, n_b, and n_c for $z>0$) behave like acceptors. Furthermore, we assume that there is a donorlike charge distribution in the AlSb layer in I for $z<-L$, with a concentration N_d and a depletion length L_d. This charge layer can be attributed to the presence of intrinsic antisite donor defects in the AlSb barrier layer and these donor defects are not fully ionized due to the effect of charge depletion. N_d and L_d can be determined in the self-consistent calculation. Thus, the Schrödinger equations for an electron and a hole are coupled via the Hartree potential seen commonly by electrons and holes.

In the absence of a gate voltage applied along the growth direction, using boundary conditions $\kappa(z)dU_H(z)/dz|_{z=-\infty}=\kappa(z)dU_H(z)/dz|_{z=W_r}=0$, with $W_r=W+\Delta W_b+\Delta W_c$ in Fig. 1, we have, after integrating Eq. (6)

$$\kappa(z)\frac{dU_H(z)}{dz}=e^2\begin{cases}L(z), & \text{I}_1;\\L(z)-L_1(z), & \text{I}_2;\\L(z)-L_2(z), & \text{II};\\R(z)+R_1(z), & \text{III};\\R(z)+R_2(z), & \text{IV};\\R(z)+R_3(z), & \text{V}.\end{cases} \tag{8}$$

Here, $L(z)=\int_{-\infty}^{z}dz_1\Delta n(z_1)$, $L_1(z)=N_d(z+L+L_d)$, $L_2(z)=n_d(z+L)+N_dL_d$, $R(z)=-\int_z^{W_r}dz_1\Delta n(z_1)$, $R_1(z)=n_a(z-W)-n_b\Delta W_b-n_c\Delta W_c$, $R_2(z)=n_b(z-W-\Delta W_b)-n_c\Delta W_c$, and $R_3(z)=n_c(z-W-\Delta W_b-\Delta W_c)$. The condition $\kappa(z)dU_H(z)/dz|_{z=0^+}=\kappa(z)dU_H(z)/dz|_{z=0^-}$ gives the condition of the charge number conservation

$$N_dL_d=n_e-n_h-n_dL+n_aW+n_b\Delta W_b+n_c\Delta W_c=x_1, \tag{9}$$

with $n_e=\int_{-\infty}^{W_r}dz\ n_e(z)$ and $n_h=\int_{-\infty}^{W_r}dz\ n_h(z)$ being, respectively, the total electron and hole density in the system.

Using the condition that $U_H(z)$ should continue at each interface and $U_H(-\infty)=0$ and $U_H(W_r)=0$, the Hartree potential is obtained, after integrating Eq. (8), as

$$U_H(z)=e^2\begin{cases}Q_L(z), & \text{I}_1;\\Q_L(z)-Q_1(z), & \text{I}_2;\\Q_L(z)-Q_2(z), & \text{II};\\Q_R(z)+Q_3(z), & \text{III};\\Q_R(z)+Q_4(z), & \text{IV};\\Q_R(z)+Q_5(z), & \text{V}.\end{cases} \tag{10}$$

Here, $Q_L(z)=\int_{-\infty}^{z}dz_1\kappa^{-1}(z_1)\int_{-\infty}^{z_1}dz_2\Delta n(z_2)$, $Q_1(z)=N_d(z+L+L_d)^2/2\kappa_1$, $Q_2(z)=n_d(z+L)^2/2\kappa_2+N_dL_d[(z+L)/\kappa_2+L_d/\kappa_1]$, $Q_3(z)=n_a(z-W)^2/2\kappa_3+n_b\Delta W_b[\Delta W_b/2\kappa_1+(W-z)/\kappa_3]+n_c\Delta W_c[(W+\Delta W_c/2-z)/\kappa_3+\Delta W_b/\kappa_1]$, $Q_4(z)=n_b(z-W-\Delta W_b)^2/2\kappa_1+n_c\Delta W_c[\Delta W_c/2\kappa_3+(W+\Delta W_b-z)/\kappa_1]$, $Q_5(z)=n_c(z-W_r)^2/2\kappa_3$, and $Q_R(z)=\int_z^{W_r}dz_1\kappa^{-1}(z_1)\int_{z_1}^{W_r}dz_2\Delta n(z_2)$. Using a condition $U_H(0^+)=U_H(0^-)$, we obtain

$$N_dL_d(L/\kappa_3+L_d/2\kappa_1)=x_2, \tag{11}$$

with

$$x_2=Q_L(0)-Q_R(0)-\frac{n_aW^2}{2\kappa_3}-n_b\Delta W_b\left(\frac{\Delta W_b}{2\kappa_1}+\frac{W}{\kappa_3}\right)-n_c\Delta W_c\left(\frac{W+\Delta W_c/2}{\kappa_3}+\frac{\Delta W_b}{\kappa_1}\right)-\frac{n_dL^2}{2\kappa_2}.$$

Thus, from Eq. (9) and Eq. (11), the depletion length and donor charge density in an AlSb layer in I are obtained, respectively, as

$$L_d=2\kappa_1(x_2/x_1-L/\kappa_3)\quad\text{and}\quad N_d=x_1/L_d. \tag{12}$$

The carrier distribution is

$$n_i(z) = \sum_n N_n^i |\psi_n^i(z)|^2, \tag{13}$$

with N_n^i being the carrier density in the nth subband. Taking the electron (hole) effective mass in the InAs (GaSb) well layer as the density-of-states (DoS) mass for electrons (holes) and assuming a constant Fermi level E_F across the sample, at low temperatures (i.e., $T \to 0$) we have

$$N_n^e = \frac{m_2^e}{\pi\hbar^2}\Theta(E_F - \varepsilon_n^e)(E_F - \varepsilon_n^e), \tag{14}$$

and

$$N_n^h = \frac{m_3^h}{\pi\hbar^2}\Theta(\varepsilon_n^h - E_F)(\varepsilon_n^h - E_F). \tag{15}$$

The total electron or hole density in the system is then $n_i = \Sigma_n N_n^i$.

By solving the above-mentioned equations self-consistently, we can obtain the electronic properties of interest (e.g., electron/hole wave functions and subband energies, total confining potential energies for electrons and holes, electron/hole density in different subbands, total electron/hole density, charge distributions, depletion length, etc.) by using the known material parameters (e.g., effective masses for an electron and a hole, dielectric constants, conduction and valance band offsets, etc.) and known sample-growth parameters (e.g., the widths of the InAs and GaSb well layers, the background impurity concentrations in different layers, etc.). It should be noted that in the calculation, we need to determine the Fermi energy E_F as the only input parameter. We assume that the Fermi level of the sample system is pinned around the average bonding level for bulk donor defects in the AlSb (GaSb) barrier layer. The results obtained from photoemission experiments[16] indicated that the average bonding energy for the intrinsic bulk donors in GaSb is about 0.1 eV. Thus, we assume that when $\Delta W_c \leq 50$ nm, the E_F is pinned at the donor level $E_F = E_F^0 \sim 110$ meV. When $\Delta W_c > 50$ nm, $E_F = E_F^0 + \Delta W_c(-2.5\times 10^{-4} + 5\times 10^{-7}\Delta W_c)$ where E_F is in meV and ΔW_c is in nanometer. A slight variation of E_F for a large cap layer thickness is mainly caused by band bending due to the injection of holes from the cap layer.

III. NUMERICAL RESULTS AND DISCUSSIONS

In the calculation, we take the material parameters for AlSb, InAs, and GaSb as follows. (1) The effective mass [see Fig. 1 and Eq. (1)]: $m_1^e = 0.12 m_e$, $m_2^e = 0.038 m_e$, $m_3^e = 0.04 m_e$, $m_1^h = 0.98 m_e$, $m_2^h = 0.40 m_e$, and $m_3^h = 0.33 m_e$ with m_e being the mass for a rest electron. (2) The static dielectric constant: $\kappa_1 = 17.76$, $\kappa_2 = 15.15$, and $\kappa_3 = 15.69$. (3) The conduction- and valence-band offsets are indicated in Eq. (4). In conjunction with sample devices used in experiments,[15] we take (see Fig. 1) $L = 17$ nm, $W = 5$ nm, and $\Delta W_b = 30$ nm and assume $n_d = n_a = n_b = 10^{15}$ cm^{-3} and $n_c = 3\times 10^{15}$ cm^{-3}. Different samples in the experiments correspond to different widths of the GaSb cap layers ΔW_c.[15] It should be noted that in InAs/GaSb-based T2BG-QW systems, the confinement for electrons and holes is much stronger than that in III-V based QWs [see, Eq. (4)]. Together with the fact that in the experiments[15] the InAs well layer is wider than the GaSb well layer, only the heavy-hole states in the GaSb well layer are occupied by holes. Thus, we only include heavy holes in different layers within the calculation.

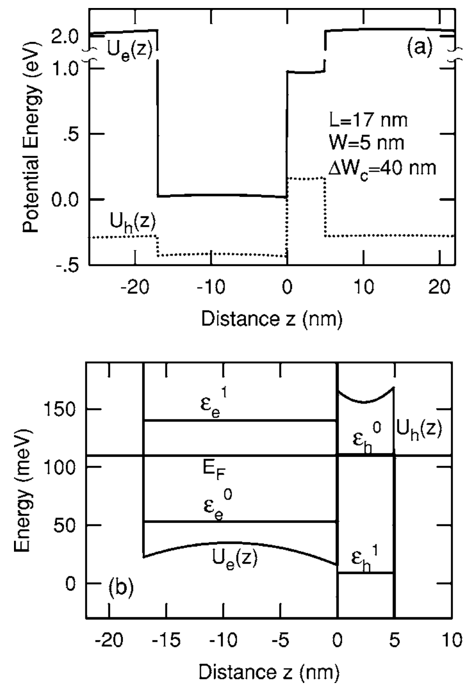

FIG. 2. (a) Potential profile of the conduction and valence band [$U_e(z)$ and $U_h(z)$] along the growth direction of an InAs/GaSb-based type II and broken-gap QW and (b) the positions of two lowest electron subbands (ε_0^e and ε_1^e) and two highest hole subbands (ε_0^h and ε_1^h) along with the Fermi energy E_F.

In Fig. 2, we show in (a) the profile of the confinement potential to electrons $U_e(z)$ and holes $U_h(z)$ in an InAs/GaSb-based T2BG-QW indicated schematically in Fig. 1 and in (b) the energies of two lowest electron subbands and two highest hole subbands along with the Fermi energy. These results are presented for $L = 17$ nm, $W = 5$ nm, and $\Delta W_c = 40$ nm. We see that in such a case, the lowest electron subband in the InAs well layer and the highest hole subband in the GaSb well layer are occupied, respectively, by electrons and holes and $\varepsilon_0^h - \varepsilon_0^e \simeq +58$ meV. Therefore, a type II and broken-gap structure is achieved in this sample structure. With these sample-growth parameters, we find that the maximum energy of the Hartree potential plus exchange potential is about 35 meV [see Fig. 2(b)]. This energy is much smaller than the confining potential energy which is about 2000 meV for electrons and about 600 meV for holes. Hence, the band bending induced by these many-body effects are not very strong in such structures in comparison with the confining potentials induced by band-edge discontinuities. We notice that when $L = 17$ nm and $W = 5$ nm, the Fermi level of the system is very close to ε_0^h ($\varepsilon_0^h - E_F \simeq 1.1$ meV). This is the main reason why the hole density in the system is much smaller than the electron density.

For application of T2BG-QW systems as electronic and optical devices, it is necessary to know the overlap of electron and hole wave functions at the interface between InAs and GaSb well layers. In Fig. 3, we show the wave functions for two lowest electron subbands and two highest hole sub-

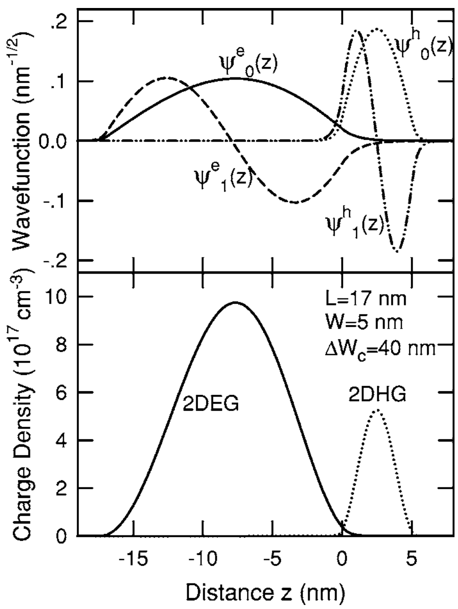

FIG. 3. Wave functions (upper panel) for two lowest electron subbands $[\psi_0^e(z)$ and $\psi_1^e(z)]$ and two highest hole subbands $[\psi_0^h(z)$ and $\psi_1^h(z)]$ and charge distribution (lower panel) for 2DEG and 2DHG along the growth direction. Note that the InAs layer is in $[-17,0]$ nm and the GaSb layer is in $[0,5]$ nm.

bands (upper panel) and electron and hole distribution (lower panel) along the growth direction. We see that when $L=17$ nm and $W=5$ nm, (i) the electrons and holes are located mainly in, respectively, the InAs and GaSb well layers; (ii) there is a rather significant overlap of the electron and hole wave functions at the interface between InAs and GaSb; and (iii) because of much heavier effective-mass for holes in the GaSb layer, hole distribution is more localized than electron distribution. As a result, the overlap between the electron and hole distributions and wave functions is mainly through the penetration of the electron wave functions into the GaSb layer. In such a structure, because of higher electron density and wider InAs well layer, electron distribution is more pronounced than hole distribution along the growth direction. It has been demonstrated both experimentally and theoretically that in a T2BG-QW, the overlap of the electron and hole wave functions at the interface can lead to a minigap in the electron and hole dispersion relations and, as a result, a giant negative magnetoresistance.[17] We note that in a T2BG-QW, the overlap of the electron and hole wave functions in the system implies an enhancement of the *attractive* force between two spatially separated layers. Consequently, the energy gap induced by attractive many-body interaction can be enhanced in the electron and hole dispersion relations. Using the electron and hole wave functions obtained from this self-consistent calculation, we can calculate the enhancement of the minigap or coupling energy induced by the Coulomb potential using a state-of-the-art many-body theory.[18] However, the calculation of the minigap in the energy dispersion needs further theoretical work considerably and we do not attempt it in the present work.

In Fig. 4, we plot the total electron and hole densities in the system as a function of the GaSb cap width ΔW_c at the fixed InAs and GaSb well thicknesses $L=17$ nm and $W=5$ nm. The results obtained from the self-consistent calculation (circles) are compared with those measured experimentally (triangles).[15] With increasing GaSb cap width ΔW_c, the electron density decreases slightly and the hole density first increases then decreases, in line with experimental findings.[15] The theoretical results confirm an important experimental scheme that a GaSb cap layer with a width ΔW_c in Fig. 1 can provide an extra source of charges to vary the electronic subband structure of the device system. Because of much heavier effective-mass for holes in the GaSb well layer, the hole density [see Eq. (15)] depends more strongly on the cap layer width which results in a further bending of the confining potentials on top of the Hartree and exchange potentials induced by electron and hole distributions.

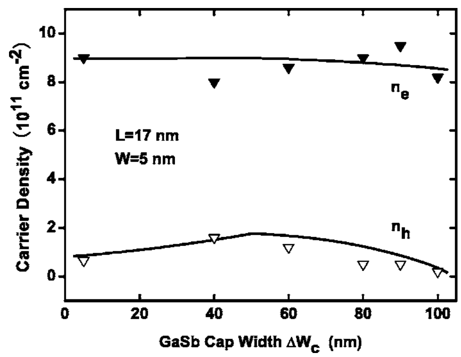

FIG. 4. Electron (n_e) and hole (n_h) densities as a function of GaSb cap layer thickness ΔW_c at the fixed InAs and GaSb well widths ($L=17$ nm and $W=5$ nm). The solid curves are obtained from the self-consistent calculation and the solid and open triangles are measured experimentally (Ref. 15).

To gain a more detailed understanding of the effects of a GaSb cap layer on electronic subband structure of an InAs/GaSb heterostructure, in Fig. 5 we show the electron and hole subband energies (upper panel) and donor charge density and depletion length in the AlSb barrier layer as a function of the GaSb cap width. Because we have assumed that

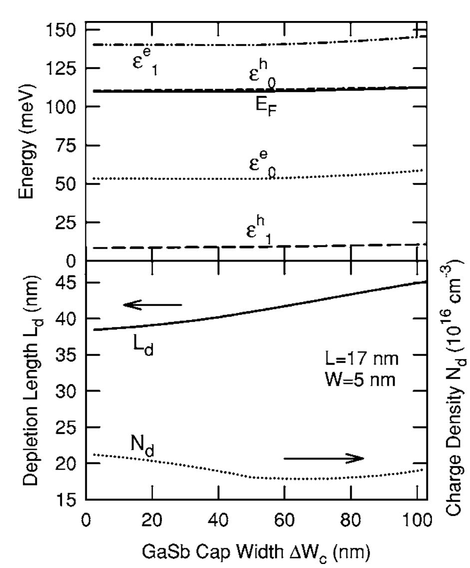

FIG. 5. Electron and hole subband energies (ε_j^e and ε_j^h along with the Fermi energy E_F in upper panel) and the depletion length L_d and donor concentration N_d in the AlSb barrier layer (lower panel) as a function of GaSb cap width ΔW_c at the fixed InAs and GaSb well widths ($L=17$ nm and $W=5$ nm).

the impurities in the GaSb cap layer are acceptorlike, the Hartree potential induced by charges in this layer is positive. As a result, the band bending induced by the GaSb cap layer is upwards and, consequently, the electron and hole subband energies increase slightly with the GaSb cap width ΔW_c. This is the main reason why the electron density decreases slightly with increasing ΔW_c as shown in Fig. 4. When $\Delta W_c < 50$ nm, the hole density increases with ΔW_c because more holes are injected into the GaSb well from the cap layer. When $\Delta W_c > 50$ nm, the upwards band bending induced by acceptorlike charges in the cap layer pushes the Fermi level closer to the highest hole subband [i.e., $\varepsilon_0^h - E_F$ in Eq. (15) becomes slightly smaller]. As a result, the hole density decreases with ΔW_c when $\Delta W_c > 50$ nm as shown in Fig. 4. We find that the concentration of donorlike defects in the AlSb barrier layer $N_d \sim 2\times 10^{17}$ cm^{-3} depends rather weakly on ΔW_c. With increasing ΔW_c, more acceptor charges are injected into the structure so that the depletion length for the donor impurities in the AlSb barrier layer increases in order to satisfy the condition of the charge number conservation in the system. Depletion of holes from the GaSb cap layer by surface defects at the cap layer/oxide interface can account for the increased acceptor charge with increasing ΔW_c resulting in a surface band bending potential E_F^S, which is defined as the position of the Fermi level E_F, relative to the top of the valence band at the GaSb cap layer surface. Experimental results[15] confirm the band bending effect of surface depletion on the electronic properties of the structure and show that E_F^S, which can be estimated by $E_F^S \sim en_c(\Delta W_c)^2/(2\kappa_3)$, is pinned for cap widths greater than around 90 nm. The above expression for the slight variation of E_F for $\Delta W_c > 50$ nm, accounts for the combined band bending effects of the GaSb cap layer in the GaSb quantum well region.

In this work, the main theoretical assumption is made on the basis that there are intrinsic antisite defects in the AlSb barrier layer, which can provide the source of ionized donors for undoped InAs/GaSb quantum wells and pin the Fermi level of the system around the average bonding energy of bulk intrinsic defects. With increasing the GaSb cap layer thickness, more holes are injected into the system and an extra band bending can be achieved. Although the band bending induced by the presence of the GaSb cap layer is rather weak, it can cause a slight change of the Fermi energy of the system and affect the hole density significantly due to its heavy effective mass. This assumption leads to an agreement of the corresponding theoretical results with those obtained experimentally for undoped sample structures. Thus, we can utilize the theoretical results for the understanding of the experimental findings. The results obtained from the proposed self-consistent calculation indicate that the ionized donor concentration in the AlSb barrier layer is about 2×10^{17} cm^{-3} (a very reasonable value for intrinsic or background defects induced during the MBE growth) and depends weakly on the presence of the GaSb cap layer. As a result, the impurity states in the AlSb barrier layer adjacent to the InAs well layer are quite stable. This implies further that the intrinsic antisite defects in the AlSb barrier layer can provide high density of electrons in the InAs well layer and pin the Fermi level of the heterostructure.

IV. CONCLUDING REMARKS

In this article, we have presented the theoretical component of a combined experimental and theoretical investigation on electronic properties of InAs/GaSb-based QW systems.[15] A simple and transparent theoretical approach has been developed to study the electronic subband structure of InAs/GaSb-based type II and broken-gap quantum well systems. The theoretical considerations have been made in conjunction with experimental sample systems and the corresponding findings. The calculations have been carried out on the basis of solving self-consistently the Schrödinger equation for electron/hole wave functions and energy spectra and the Poisson equation for confining potentials. We have examined the dependence of the electronic properties in such systems on sample growth parameters such as the GaSb cap width and compared the obtained results with those measured experimentally. The main conclusions drawn from this study are summarized as follows.

With the known material coefficients and known sample-growth parameters, the electronic subband structure of an InAs/GaSb-based type II and broken-gap quantum well system can be evaluated by using the proposed self-consistent calculation. The results obtained from such calculation can reproduce those observed experimentally and be used for understanding of the experimental findings.

The theoretical results have confirmed an experimental scheme that in a undoped InAs/GaSb heterostructure, a GaSb cap layer can provide an extra source of charges to alter electronic subband structure of the sample system. The presence of such a cap layer can inject holes into the structure and result in a slight upwards bending of the band-edges due to the introduction of the Hartree potential. With increasing the cap width, the electron density decreases slightly (due to the upwards band bending) and the hole density first increases (because more holes are injected into the system) then decreases (owing to the upwards band bending). The hole density depends more strongly on the presence of the cap layer due to the hole's heavier effective mass. These points agree with those observed experimentally.

The results obtained from the self-consistent calculation indicate that in a undoped InAs/GaSb heterostructure, the impurity states in the AlSb barrier layer adjacent to the InAs well layer are quite stable, where the donor concentration depends weakly on the presence of the GaSb cap layer and the depletion length of these donor defects increases slightly with the GaSb cap width. These results suggest that the intrinsic antisite bulk defects in the AlSb barrier layer can provide high density of electrons in the InAs well layer and pin the Fermi level of the system around the average bonding energy of these donorlike impurities, in agreement with experimental results.

The InAs/GaSb-based type II and broken-gap QW systems without intentional doping can achieve high electronic mobility (~ 10 m^3/V s) and high carrier density (n_e

$\sim 10^{12}$ cm^{-2}).[15] These sample coefficients are very important for the applications of such systems as novel and advanced electronic and optical devices. The electronic subband structure obtained from the proposed self-consistent calculation can also be used for further calculation of the transport, optical, and optoelectronic properties of the InAs/GaSb heterostructures. We hope that our recent experimental measurements[15] and present theoretical calculations in this paper can help to gain an in-depth understanding of these unique quantum well structures.

ACKNOWLEDGMENTS

One of us (W.X.) was supported by the Australian Research Council and Chinese Academy of Sciences.

[1]M. Altarelli, Phys. Rev. B **28**, 842 (1983).
[2]H. Munekata, J. C. Maan, L. L. Chang, and L. Esaki, J. Vac. Sci. Technol. B **5**, 809 (1987).
[3]See, e.g., Ikai Lo, W. C. Mitchel, S. Elhamri, R. S. Newrock, and R. Kaspi, Appl. Phys. Lett. **65**, 1024 (1994).
[4]See, e.g., J.-P. Cheng, J. Kono, B. D. McCombe, Ikai Lo, W. C. Mitchel, and C. E. Stutz, Phys. Rev. Lett. **74**, 450 (1995).
[5]See, e.g., R. Magri, L. W. Wang, A. Zunger, I. Vurgaftman, and J. R. Meyer, Phys. Rev. B **61**, 10235 (2000).
[6]E. Halvorsen, Y. Galperin, and K. A. Chao, Phys. Rev. B **61**, 16743 (2000).
[7]X. F. Wei, W. Xu, and Z. Zeng, J. Phys. Condens. Matter **19**, 026216 (2007).
[8]M. Altarelli, U. Ekenberg, and A. Fasolino, Phys. Rev. B **32**, 5138 (1985).
[9]A. Zakharova, S. T. Yen, and K. A. Chao, Phys. Rev. B **66**, 085312 (2002).
[10]W. Xu and J. Mahanty, J. Phys. Condens. Matter **6**, 4745 (1994).
[11]W. Xu, Int. J. Mod. Phys. B **10**, 1293 (1996).
[12]W. Xu, Phys. Rev. B **51**, 9770 (1995).
[13]W. Xu, Phys. Rev. B **50**, 14601 (1994).
[14]P. A. Folkes, G. Gumbs, and W. Xu, J. Appl. Phys. **92**, 632 (2002).
[15]P. A. Folkes, G. Gumbs, W. Xu, and M. Taysing-Lara, Appl. Phys. Lett. **89**, 202113 (2006).
[16]W. E. Spicer, I. Lindau, P. Skeath, C. Y. Su, and P. Chye, Phys. Rev. Lett. **44**, 420 (1980).
[17]M. Lakrimi, S. Khym, R. J. Nicholas, D. M. Symons, F. M. Peeters, N. J. Mason, and P. J. Walker, Phys. Rev. Lett. **79**, 3034 (1997).
[18]See, e.g., R. D. Mattuck, *A Guide to Feynman Diagrams in the Many-Body Problem* (McGraw-Hill, New York, 1976).